Recent results on the production of hadronic resonances with ALICE at the LHC

38th Winter Workshop on Nuclear Dynamics (WWND 2023)

Bong-Hwi Lim
for the ALICE Collaboration
Universita di Torino and INFN

February 8, 2023

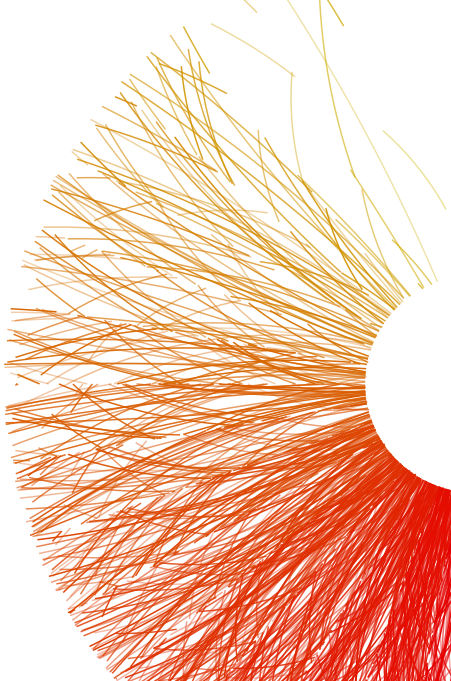

Hadronic resonances in ALICE

- **Short lifetime** comparable to the one of the hadron gas phase ($\sim$ few fm/c)
  - Suitable probes to study the properties of the hadronic phase in heavy-ion collisions.
- **Excited states** of hadrons
  - Compare results to other particles that have the same (or)similar) quark content.

Resonance	$\rho(770)^0$	$\mathrm{K}(892)^{\pm}$	$\mathrm{K}(892)^0$	$\mathrm{f}_0(980)^0$	$\Sigma(1385)^{\pm}$	$\Xi(1820)^{\pm}$	$\Lambda(1520)^0$	$\Xi(1530)^0$	$\phi(1020)^0$
Quark composition	$\frac{\mathrm{u\bar{u}}+\mathrm{d\bar{d}}}{\sqrt{2}}$	$\mathrm{u\bar{s}}$, $\mathrm{\bar{u}s}$	$\mathrm{d\bar{s}}$, $\mathrm{\bar{d}s}$	unknown	uus, dds	uss	uds	uss	$\mathrm{s\bar{s}}$
τ (fm/c)	1.3	3.6	4.2	large unc.	5–5.5	8.1	12.6	21.7	46.4
Decay	$\pi\pi$	$\mathrm{K}^0_{\mathrm{S}}\pi$	$\mathrm{K}\pi$	$\pi\pi$	$\Lambda\pi$	$\Lambda\mathrm{K}$	pK	$\Xi\pi$	KK
B.R. (%)	100	33.3	66.6	46	87	unknown	22.5	66.7	48.9

Table 1: List of resonances studied in ALICE (Run1 & Run2).

Hadronic phase in Heavy-Ion Collisions

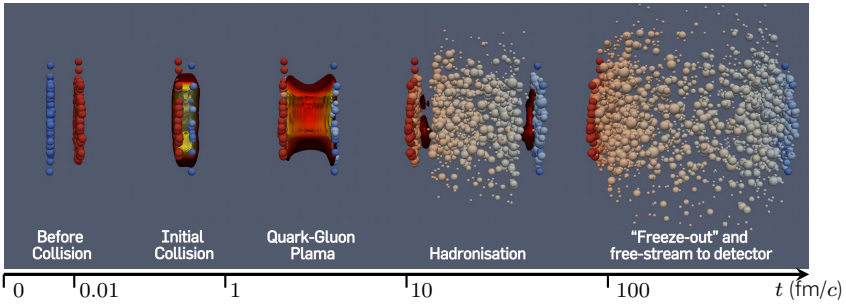

Figure 1: Simulation of the evolution of the heavy-ion collision, time flows from left to right [1]

- **Hadronic-gas phase**: between chemical freeze-out and kinetic freeze-out
  - Duration of the same order of magnitude as resonance lifetimes.

Resonances in Hadronic Phase

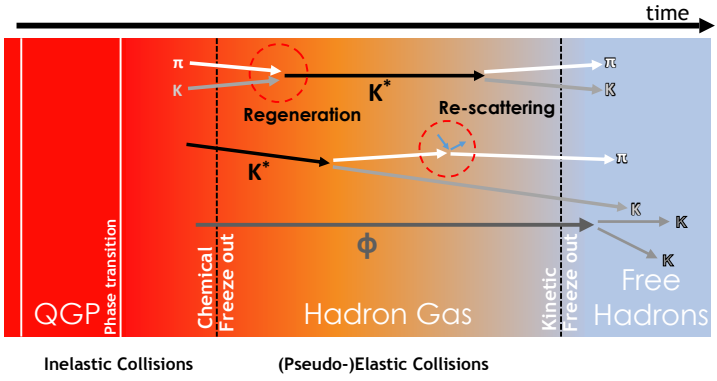

Figure 2: Sketch of interactions in hadron-gas phase. Yields of the short-lived resonance, such as K^* ($c\tau \approx 4.2$ fm), can be affected by rescattering and regeneration in hadronic phase in contrast to those of long-lived resonances, such as ϕ ($c\tau \approx 44$ fm).

- **Regeneration:**
  Pseudo-elastic scattering of decay products
  → Increase in resonance measured yield
- **Rescattering:**
  Elastic scattering smears out mass peak
  → Resonance can not be reconstructed through invariant mass
  → Decrease in resonance measured yield

Features of resonances: suppression at high multiplicities

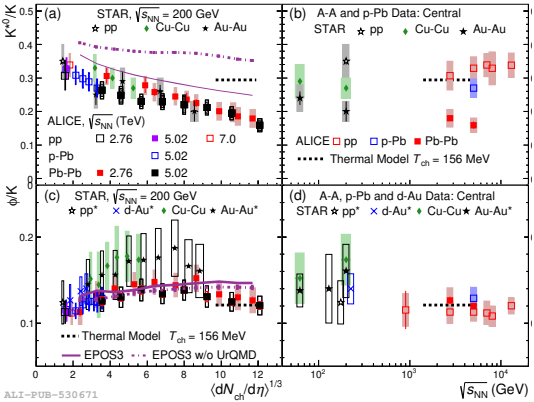

Figure 3: K^*/K and ϕ/K ratios in various collision systems and energies. (left: mulitplcity, right: energy)

- Ratio resonance yield to ground-state hadrons with similar quark content
  → K^*/K and ϕ/K ratios
- Significant suppression of K^*/K from pp to Pb–Pb
  → Presence of **hadronic interaction**: rescattering dominant effect compared to regeneration
- What drives this decrease?
  → The lifetime of the resonance
  → The cross sections for rescattering and regeneration processes
  → The time duration of the hadronic phase

The ALICE detector

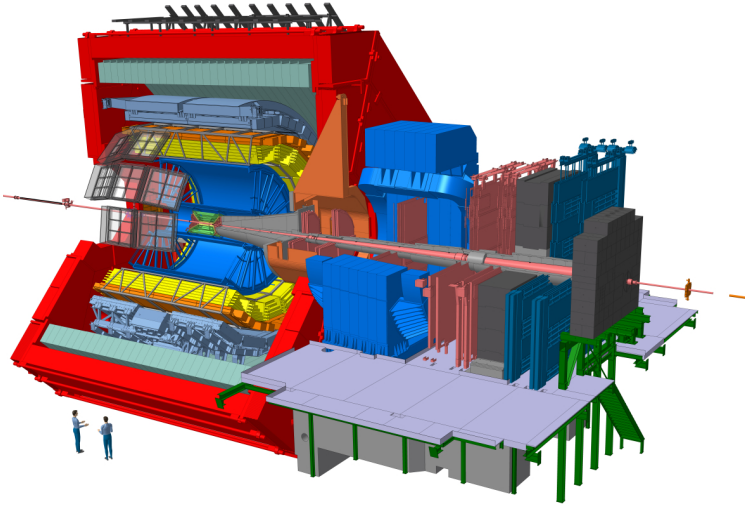

- Multi-purpose detector at the LHC with unique **particle identification** capabilities and tracking down to **very low momenta**
- Central barrel detectors ($|\eta| < 1$)

ITS: Silicon detector for tracking and vertexing

TPC: Time Projection Chamber for particle identification and tracking

TOF: Time Of Flight detector for particle identification

V0: scintillator detector for trigger and multiplicity estimation

Figure 4: Schematic view of the ALICE detector

Resonance reconstruction: analysis strategy

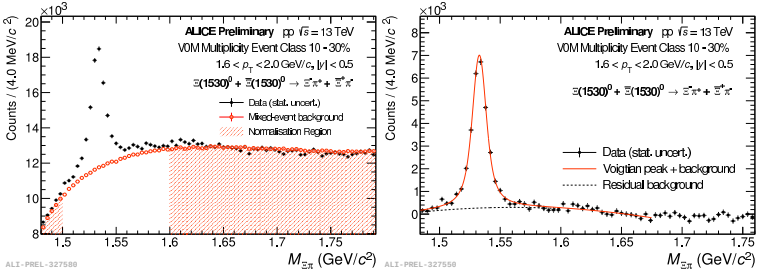

Figure 5: Invariant mass distribution of Ξ^{*0} with background (left) and fitted signal after the background subtraction (right)

- Resonances are reconstructed via the **invariant-mass technique** $M_{\mathrm{inv}} = \sqrt{(E_1 + E_2)^2 - (\vec{p_1} + \vec{p_2})^2}$
- **Uncorrelated background** is calculated via event mixing or like-sign techniques
- PID from TPC, TOF for the daughter tracks, V0 or Cascade topology for $\mathrm{K}^0_{\mathrm{s}}$, Λ, $\Xi^{\pm}$
- **Residual background**: Correlated pairs or misidentified decay products, usually modeled by a polynomial function
- **Signal**: Breit-Wigner or Voigtian function

Invariant mass distribution of various resonances#1

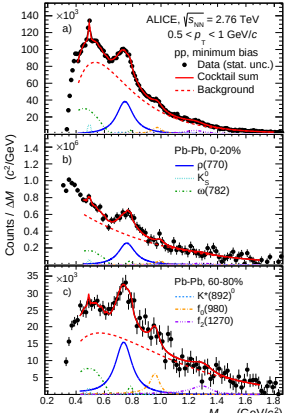

Figure 6: $\rho(770)$ [2]

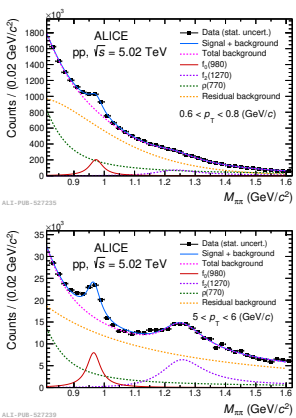

Figure 7: $f_0(980)$ [3]

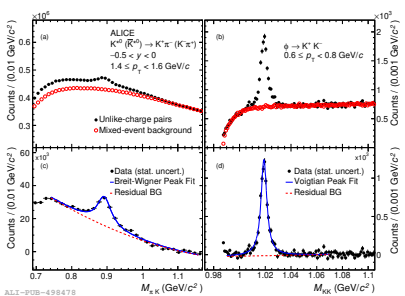

Figure 8: $K(892)^0$ and $\phi(1020)$ [4]

Invariant mass distribution of various resonances#2

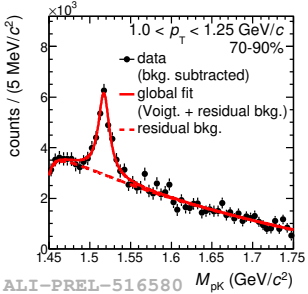

Figure 9: $\Lambda(1520)^0$ [5]

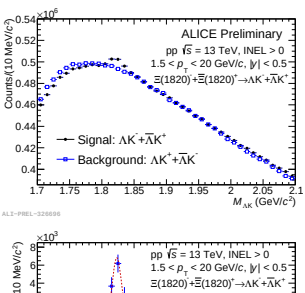

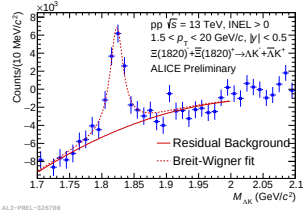

Figure 10: $\Xi(1820)$

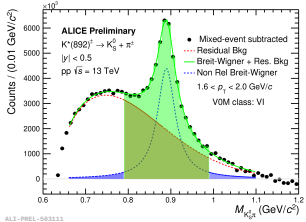

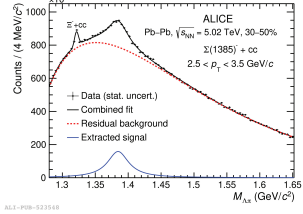

Figure 11: $\mathrm{K}(892)^{\pm}$ and $\Sigma(1385)^{\pm}$ [6]

Transverse momentum (p_{T}) spectra

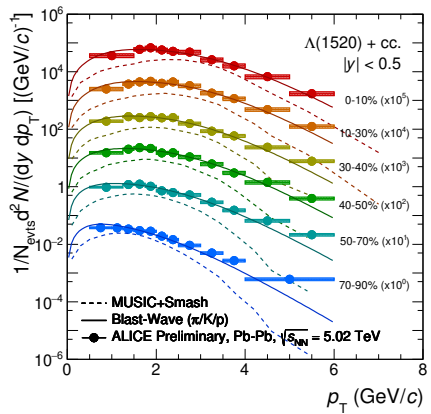

Figure 12: $\Lambda(1520)^0$ p_{T} spectra

- p_{T} spectra obtained for different centralities classes (multiplicity classes for pp collisions)
- Hardening of spectra with increasing centrality of the collision

  → Caused by radial flow.
- Comparison with hydrodynamic models:

  → Spectral shapes are in agreement with Blast- Wave model (from π, K, p)

  → MUSIC [7] hydrodynamic models with SMASH afterburner underestimates the $\Lambda(1520)$ yield

Integrated yields $\mathrm{d}N/\mathrm{d}y$

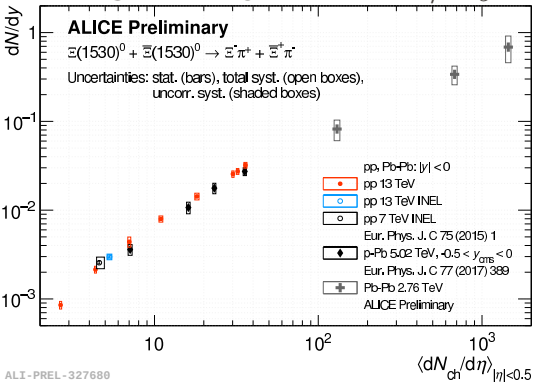

Figure 13: $\Xi(1530)^0\ \mathrm{d}N/\mathrm{d}y$

- Resonance production is driven by the multiplicity.

  It doesn't depend on the system size or the centre-of-mass energy

Mean transverse momentum $\langle p_{\mathrm{T}} \rangle$

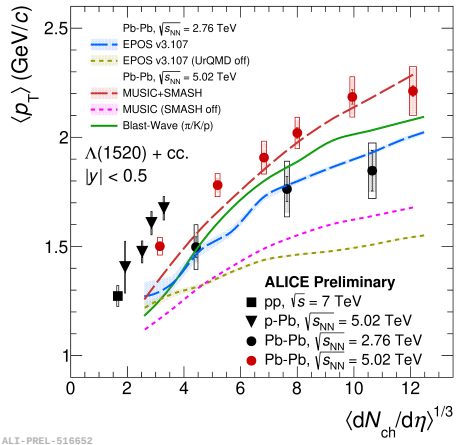

Figure 14: $\Lambda(1520)^0$ $\langle p_{\mathrm{T}} \rangle$

- Mean transverse momentum provides first-order characterization of the spectral shapes.
- $\langle p_{\mathrm{T}} \rangle$ values increase with increasing multiplicity and are higher for the higher centre-of-mass energy
- Models that do not include a hadronic afterburner (SMASH) do not reproduce the data

  → MUSIC [7] without SMASH and EPOS3 without UrQMD afterburner [8] underestimate the trend

Particle ratio: $\mathrm{K}(892)^{\pm}/\mathrm{K}^{0}_{\mathrm{s}}$

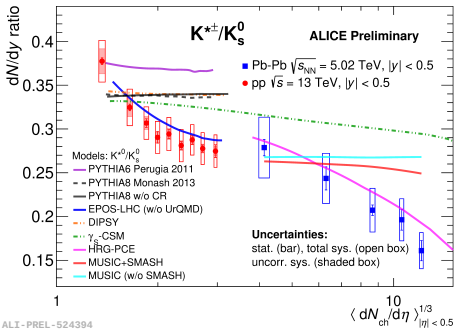

Figure 15: $\mathrm{K}(892)^{\pm}/\mathrm{K}^{0}_{\mathrm{s}}$

- The trend of the particle ratio is similar to the one of $\mathrm{K}(892)^{0}/\mathrm{K}$
- Suppression in central Pb-Pb collisions (AA collisions)
- EPOS-LHC [9] model: describes the measurements qualitatively in small systems.
- HRG [10] model: describes the measurements both qualitatively and quantitatively.

Particle ratio: $\Lambda(1520)^0/\Lambda$

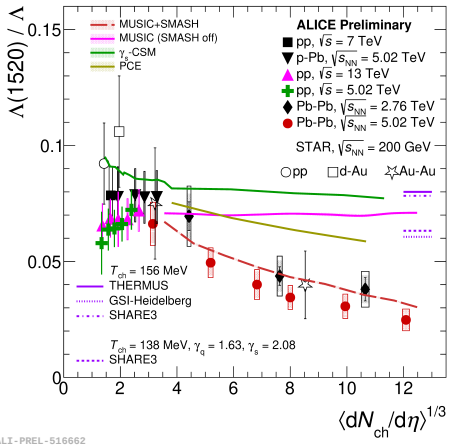

Figure 16: $\Lambda(1520)^0/\Lambda$

- Gradual decrease of the p_{T}-integrated $\Lambda(1520)^0/\Lambda$ yield ratio from peripheral to central Pb–Pb collisions
- Thermal models [10, 11] overestimate the data
- MUSIC + SMASH [7] reproduces the multiplicity suppression trend
- Small systems:
  →Small systems: no suppression observed.

Particle ratio: $\Sigma(1385)^{\pm}/\pi$

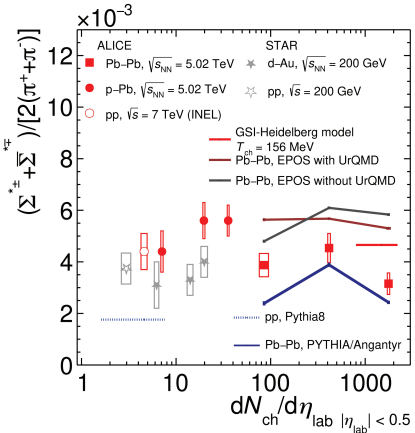

Figure 17: $\Sigma(1385)^{\pm}/\pi$

- Hint of suppression with respect to the thermal model is observed in central collisions
  → Future higher precision measurements are needed to confirm the trend
- EPOS3 with UrQMD [8] qualitatively describes the data but overestimates the yield ratios in all collision centralities.

Particle ratios in a nut shell

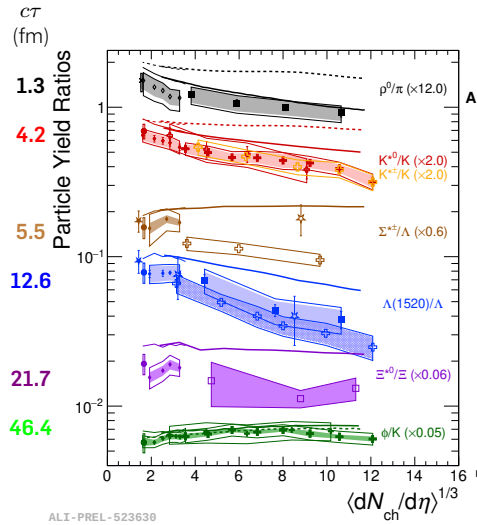

- Long-living resonances, $\Xi(1530)^0$ and ϕ show a **flat behaviour** with system size within the uncertainties

  → $\langle \mathrm{d}N_{\mathrm{ch}}/\mathrm{d}\eta \rangle^{1/3}$: Proxy for the system size [12]

- $\Lambda(1520)^0$ is **suppressed** more than the $\mathrm{K}(892)$ in central collisions

  → Regeneration may play a more important role in $\mathrm{K}(892)$ than in $\Lambda(1520)^0$?

ϕ meson pair production #1

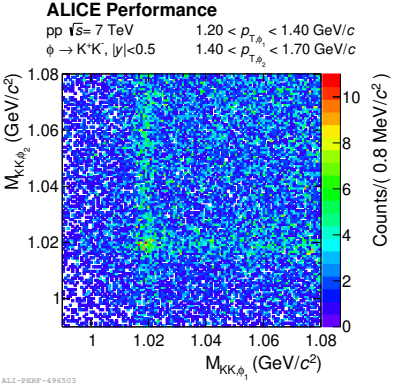

Figure 18: 2D Invariant mass histogram of two ϕ candidates

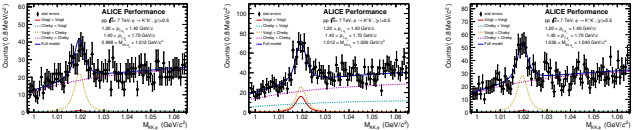

Figure 19: Conditional signal extraction for different invariant mass ranges

- **Strangeness enhancement in small systems**
  → Canonical thermal model describes the strangeness enhancement very well while couldn't describe the ϕ/π ratio.
- Main goal: is ϕ production purely statistical? or modulated? (enhanced or suppressed)
  $< Y_{\phi\phi} >$: Inclusive ϕ pairs production
  $\sigma^2_\phi = 2 < Y_{\phi\phi} > + < Y_\phi > - < Y_\phi >^2$: Variance
  $\gamma_\phi = \frac{\sigma^2_\phi}{< Y_\phi >} - 1 = 2\frac{< Y_{\phi\phi} >}{< Y_\phi >} - < Y_\phi >$

ϕ meson pair production #2

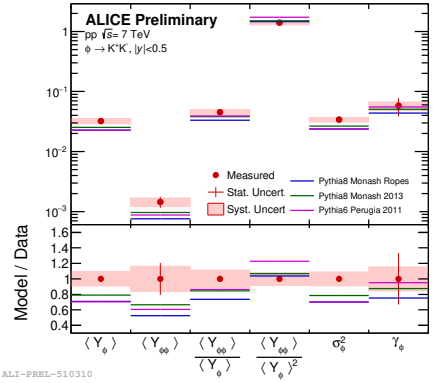

Figure 20: ϕ pair measurement results

- **Comparison to the models**: Average yield of produced ϕ and ϕ pairs, together with variance are underestimated
- New characterisation technique (γ_ϕ) hint at the accordance with the production statistics even though the integrated yields are not reproduced.
- Large statistical uncertainties $\rightarrow$ Further improve the precision of the measurement in Run3

Searching for the glueball candidates: $\mathrm{f}_2'(1525)$, $\mathrm{f}_0(1710)$

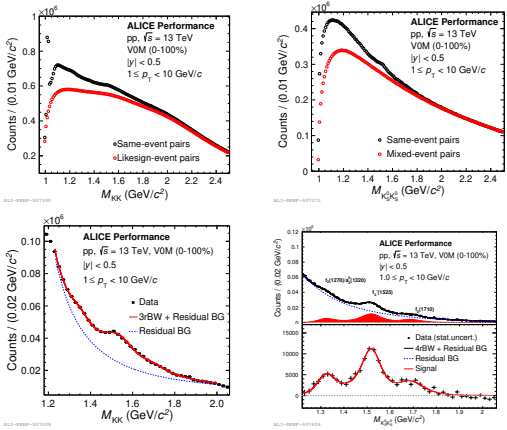

Figure 21: KK (left) and $\mathrm{K^0_S K^0_S}$ (right) invariant mass distribution (top) and fitted distribution after background subtraction (bottom)

- The possible existence of glueballs was predicted in Lattice QCD [13, 14].
- Candidates:
  - Mass range: 1550–1750 MeV/c^2
  - Total angular momentum, charge and parity: $J^{PC} = 0^{++}$
- Decay modes KK, $\mathrm{K^0_S K^0_S}$ was searched for in pp collisions at $\sqrt{s} = 13$ TeV.
- KK ($\mathrm{K^0_S K^0_S}$) Fitted with (coherent) sum of Breit-Wigner functions + residual background.
  - KK channel: 2 invariant mass peaks are visible.
  - $\mathrm{K^0_S K^0_S}$ channel: 3 invariant mass peaks are seen.
    $\rightarrow$Consistent with the observation in ep collisions at HERA [13]
- Looking forward to Run 3 and Run 4 data for precise measurements.

Resonances in transverse spherocity classes

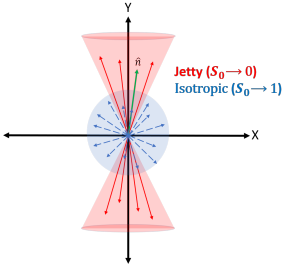

- Event shape observable: **sensitive to hard and soft proceeses**.
- Can be used to distinguish between isotropic (dominated by soft QCD) and jetty (dominated by hard QCD) events.

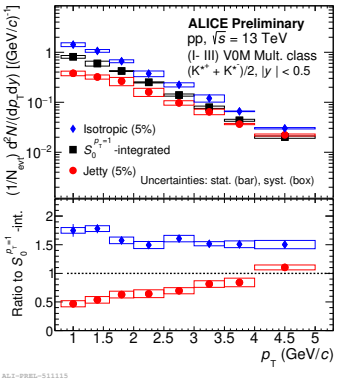

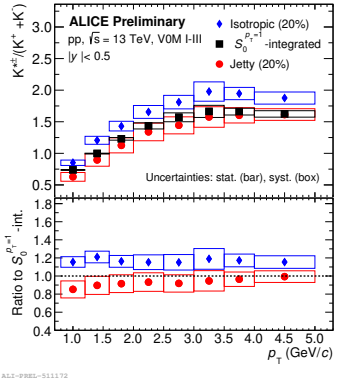

- The $\mathrm{K}(892)^{\pm}$ yield is higher in isotropic events $\rightarrow$ Harder spectra in jetty events
- $\mathrm{K}(892)^{\pm}/\mathrm{K}_{\mathrm{s}}^{0}$ ratio shows a hint of dependence on transverse spherocity.

Summary

- **Resonance** production is independent of the **collision energy** and **system** and is driven by the event **multiplicity**.
- Short-lived resonances (ρ, K^*, Σ^*, Λ^*) are suppressed in most **central** collisions.
- **Rescattering** is the dominant process in the hadronic phase for the short-lived resonances ($\tau <\sim 15$ fm/c).
- Further studies are ongoing. New multi-differential measurements, including higher-mass resonances, will be done using the higher data sample of Run3

Backup1

- Backup slide

References I

[1] MADAI collaboration, Hannah Petersen and Jonah Bernhard. https://webhome.phy.duke.edu/~jp401/music_manual/. Accessed: 2021-10-13.

[2] Shreyasi Acharya et al. "Production of the $\rho(770)^0$ meson in pp and Pb-Pb collisions at $\sqrt{s_{\mathrm{NN}}}$ = 2.76 TeV". In: Phys. Rev. C 99.6 (2019), p. 064901. DOI: 10.1103/PhysRevC.99.064901. arXiv: 1805.04365 [nucl-ex].

[3] "$\mathrm{f}_0(980)$ production in inelastic pp collisions at $\sqrt{s} = 5.02$ TeV". In: (June 2022). arXiv: 2206.06216 [nucl-ex].

[4] Shreyasi Acharya et al. "Production of K*$(892)^0$ and $\phi(1020)$ in pp and Pb-Pb collisions at $\sqrt{s_{\mathrm{NN}}} = 5.02$ TeV". In: Phys. Rev. C 106.3 (2022), p. 034907. DOI: 10.1103/PhysRevC.106.034907. arXiv: 2106.13113 [nucl-ex].

[5] Shreyasi Acharya et al. "Suppression of $\Lambda(1520)$ resonance production in central Pb-Pb collisions at $\sqrt{s_{\mathrm{NN}}}$ = 2.76 TeV". In: Phys. Rev. C 99 (2019), p. 024905. DOI: 10.1103/PhysRevC.99.024905. arXiv: 1805.04361 [nucl-ex].

[6] "$\Sigma(1385)^{\pm}$ resonance production in Pb-Pb collisions at $\sqrt{s_{\mathrm{NN}}} = 5.02$ TeV". In: (May 2022). arXiv: 2205.13998 [nucl-ex].

[7] Dmytro Oliinychenko and Chun Shen. "Resonance production in PbPb collisions at 5.02 TeV via hydrodynamics and hadronic afterburner". In: (May 2021). arXiv: 2105.07539 [hep-ph].

References II

[8] A. G. Knospe et al. “Hadronic resonance production and interaction in partonic and hadronic matter in the EPOS3 model with and without the hadronic afterburner UrQMD”. In: Phys. Rev. C 93.1 (2016), p. 014911. DOI: 10.1103/PhysRevC.93.014911. arXiv: 1509.07895 [nucl-th].

[9] T. Pierog et al. “EPOS LHC : test of collective hadronization with LHC data”. In: (2013). arXiv: 1306.0121 [hep-ph].

[10] Anton Motornenko et al. “Kinetic freeze-out temperature from yields of short-lived resonances”. In: Phys. Rev. C 102 (2 Aug. 2020), p. 024909. DOI: 10.1103/PhysRevC.102.024909. URL: https://link.aps.org/doi/10.1103/PhysRevC.102.024909.

[11] Volodymyr Vovchenko, Benjamin Dönigus, and Horst Stoecker. “Canonical statistical model analysis of $p-p$, p-Pb, and Pb-Pb collisions at energies available at the CERN Large Hadron Collider”. In: Phys. Rev. C 100 (5 Nov. 2019), p. 054906. DOI: 10.1103/PhysRevC.100.054906. URL: https://link.aps.org/doi/10.1103/PhysRevC.100.054906.

[12] Jaroslav Adam et al. “Centrality dependence of pion freeze-out radii in Pb-Pb collisions at $\sqrt{s_{NN}} = 2.76$ TeV”. In: Phys. Rev. C 93.2 (2016), p. 024905. DOI: 10.1103/PhysRevC.93.024905. arXiv: 1507.06842 [nucl-ex].

References III

[13] S. Chekanov et al. "Inclusive $K^0_S K^0_S$ Resonance Production in ep Collisions at HERA". In: Phys. Rev. Lett. 101 (11 Sept. 2008), p. 112003. DOI: 10.1103/PhysRevLett.101.112003. URL: https://link.aps.org/doi/10.1103/PhysRevLett.101.112003.

[14] P A Zyla et al. "Review of Particle Physics, 2020-2021. RPP". In: PTEP 2020.8 (2020), 083C01. 2093 p. DOI: 10.1093/ptep/ptaa104. URL: https://cds.cern.ch/record/2729066.